Providing 5G Coverage Using Optical Methods for Terahertz Frequencies

Suresh Singh
Department of Computer Science
Portland State University
Portland, USA
email: singh@cs.pdx.edu

***Abstract*—This paper studies the propagation of terahertz signals (100 GHz to 2THz) when using convex lenses. The terahertz band has a great deal of unexploited spectrum and therefore is ideally suited to provide ultra-high data rates at short ranges. The peper presents a channel model for terahertz when using convex lenses at the transmitter. The model incorporates channel impairments such as molecular absorption and lens characteristics such as a Gaussian intensity distribution. The model is verified against detailed measurements conducted using a terahertz system. We show that the model is in very close agreement with the measured data.**

***Index Terms*—Coverage, terahertz, mmwave, 5G, propagation**

I. Introduction

The demand for wireless capacity is expected to continue growing for the foreseeable future as the number of applications and devices continues to increase [1]. Indeed, given the huge expected demand, *adaptive small* cells with diameters of ∼10m have been proposed for 5G. These cells can serve crowded indoor and outdoor spaces at rates in excess of Gbps/user. Another application for these high-bandwidth cells is to serve as "information hoses" for users requiring massive aperiodic data dumps [2]–[5]. A particularly interesting example of the latter application is for providing a large volume of data to autonomous vehicles as they travel along highways. For instance, a car coming into a large city for the first time will need a pre-trained neural network. We can imagine all the weights and biases of such a network being dumped into the car's memory as it passes a toll booth at the entrance to the city. A production neural network can easily consist of hundreds of millions of floating point variables. Given the short time a car is in range of a small cell, we need data rates in excess of several Gbps. These various scenarios are illustrated in Figure 1. In order to support these types of emerging applications, the network needs greatly enhanced capacity and significantly lowered latency (∼ 1 – 5 ms). Since the terahertz frequency band is barely used and has enormous free spectrum, this frequency band is being considered as a possible candidate for such future wireless systems [1], [5]. Our focus in this paper is to consider ways to support applications like those illustrated in Figure 1 by exploiting this spectrum.

This work was funded by the the NSF under award NeTS:Small:1618936

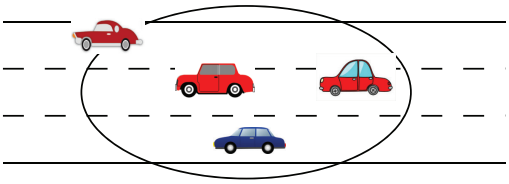

(a) Cell on highway

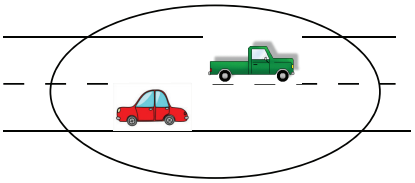

(b) Cell on roadway

(c) Cell in park

Fig. 1. Examples of small cell deployment.

The terahertz frequency band typically refers to the region from 0.1 THz to 10 THz though here we consider a smaller bandwidth up to 2 THz. This part of the spectrum is virtually unused and provides us with an opportunity to deliver data rates well in excess of terabits/sec for 5G and other wireless systems. A characteristic of this spectrum is that it is easily blocked by most common materials and some parts of the band are absorbed by water and, to a lesser degree, by oxygen or carbon dioxide. Figure 2 plots the attenuation at 1m and 10m for the spectrum up to 2 THz. As we see in the figure, some frequencies have very high attenuation which is caused

by molecular absorption[1]. This high attenuation of terahertz makes it ideally suited for short-range applications where the large attenuation enables a high degree of spatial reuse and minimal co-channel interference. Of course, the drawback of the high attenuation is the need for highly directional transmissions as well as protocols that are adapted to the *frequency selective attenuation*.

In this paper we propose using directional transmissions to create small terahertz cells. However, rather than rely on expensive MIMO arrays, we use passive lens-based systems for this purpose. Terahertz displays optical properties when it comes to propagation and can be narrowly focussed via inexpensive HDPE (High Density Poly Ethylene) lenses. Thus, a simple method to create the small cells shown in Figure 1 is to equip each access point with a lens of appropriate focal length. The terahertz signal is well confined to the cone produced by such lenses. The obvious drawback of this method is that the beam is fixed resulting in sub-optimal channels for the nodes. We note that this is not a big problem since the huge available bandwidth can be exploited to maintain high data rates despite sub-optimal access point to node channels.

The main results in this paper include a propagation model for lens based propagation of terahertz and an evaluation of this model against measurements. The remainder of the paper is organized as follows. The next section presents the lens-based model for providing coverage. Section III then presents comparisons of our model against measured data. Related work is presented in section IV and we conclude in section V.

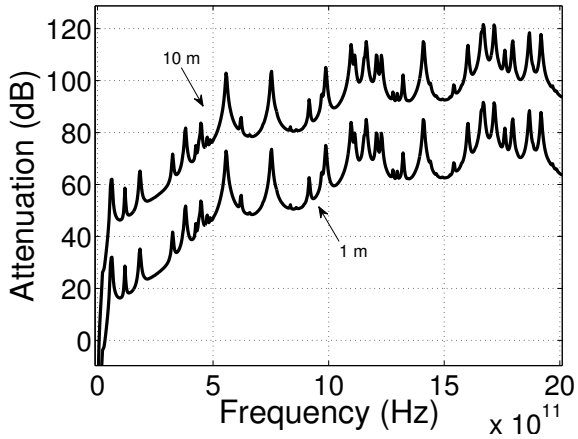

Fig. 2. Attenuation of terahertz for two distances.

II. Model

The key idea we explore in this paper is the use of lenses to create small cells and provide directional transmissions.

[1]The path loss due to frequency is $\left(\frac{c}{4\pi fr}\right)^2$ where r is the distance and path loss due to molecular absorption is $e^{-k_{abs}(f)r}$ where k_{abs} is the frequency dependent absorption constant. The total path loss is a product of these values and is frequency dependent.

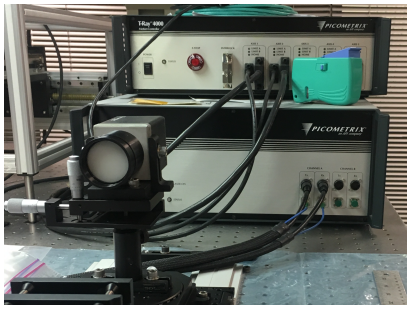

Fig. 3. Picometrix T-Ray 4000 system.

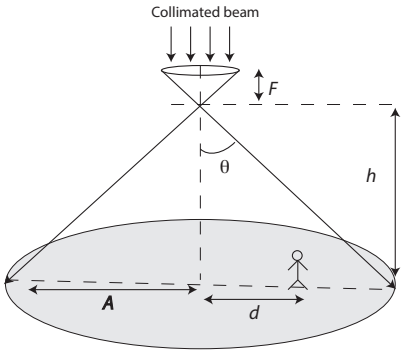

Fig. 4. Model of the lens.

The system we utilize for measurements is one such system where the transmitter and receiver are behind a HDPE lens, see Figure 3. The lens can be changed giving us the ability to produce collimated, focussed, or divergent beams. The model we consider here is using a convex lens of focal length F to create a cell of radius A as shown in Figure 4. As shown in the figure, the signal from the transmitter is a collimated beam which is then focussed at F by the lens. After that, the beam diverges and covers a circle of radius d.

A. Propagation Model

Typically, in free space wireless communications, Friis's equation [6] models the signal propagation accurately. However, as we noted previously, the terahertz channel suffers from severe atmospheric attenuation due to molecular absorption which need to be incorporated into the channel model. In previous work [7], we developed a channel model that combines Friis equation and the molecular absorption model described in [8] to obtain,

$$H(f) = \frac{\lambda}{4\pi d} \times e^{-(i2\pi f\tau + sK(f))} \quad (1)$$

where $H(f)$ is the channel transfer transfer function, s ($= \sqrt{h^2 + d^2}$ in Figure 4) is the distance travelled, τ is the propagation time, and $K(f)$ is the frequency-dependent atmospheric absorption coefficient [8]. In this paper we are primarily interested in the received signal strength and therefore, the above expression can be simplified to,

$$P_{Rx} \propto P_{Tx}\lambda^2 e^{-sK(f)} \quad (2)$$

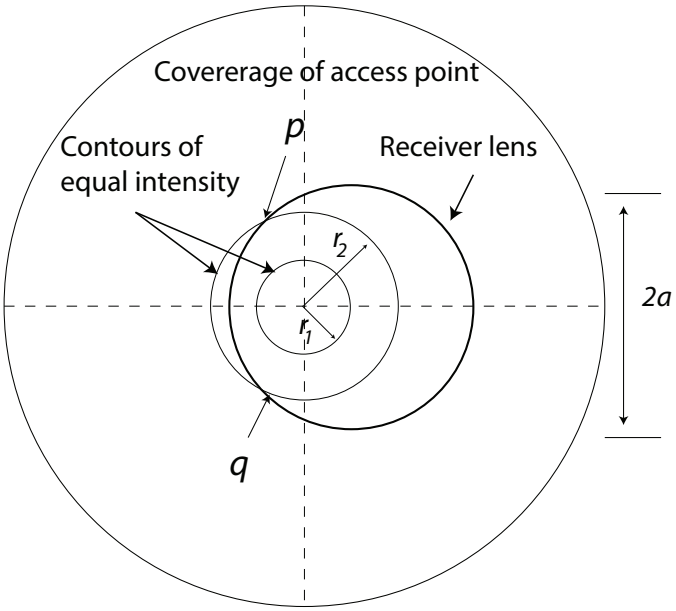

(a) Receiver offset by distance $d<a$

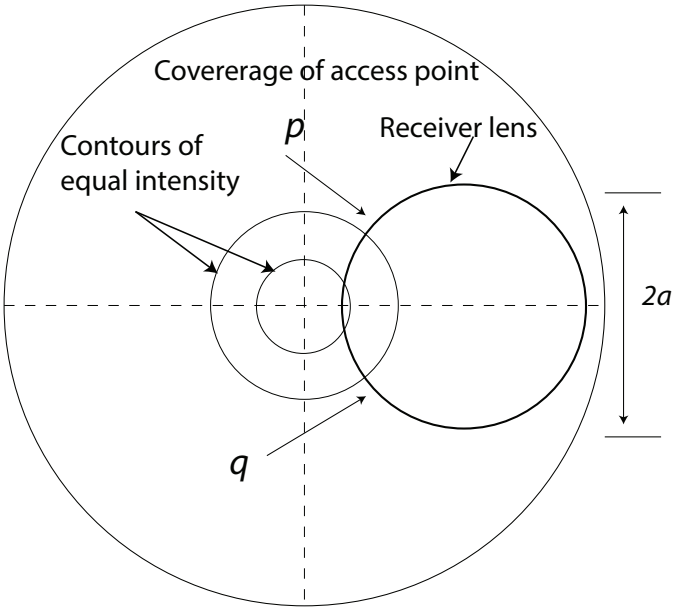

(b) Receiver offset by distance $d>a$

Fig. 5. Received power depends on lens position.

where we use proportionality instead of equality because the expression does not account for the optical effects of the lenses and for the radius of the receiver lens.

1) Lens Effects: Let us assume that the radius of the receiver lens is a. As shown in Figure 5 the receiver lens is offset by a distance of d from the center of the cell. In order to compute the received power, we need to incorporate the received power over the entire surface of the lens into equation 2 above. In an ideal case, if the signal power is uniformly distributed over the entire cell, the received power can be rewritten as,

$$P_{Rx} = \frac{a^2}{d^2} P_{Tx} \lambda^2 e^{-sK(f)}$$

Unfortunately, single convex lenses produce an intensity pattern on the image plane that is non-uniform. Indeed, the intensity pattern is most commonly modeled as Gaussion [9],

$$e = e_0 e^{-fr^2}$$

where e is the electric field intensity, r is the distance from the axis and f is the frequency. In Figure 5(a), we show two circles of constant signal intensity (with radii r_1 and r_2). For these two example contours, the signal intensity will be $e_0 e^{-fr_1^2}$ and $e_0 e^{-fr_2^2}$ respectively. *In order to obtain the total signal power falling on the receiver lens, we need to integrate the signal intensity over all the contours that intersect the lens.*

2) Complete Propagation Model: Figure 5 illustrates two cases that are distinguished by how far the receiver lens is offset relative to the center of the transmitter axis. We use d to denote this offset distance. When $d \leq a$ Figure 5(a), some portion of the receiver lens overlaps the center of the cell while when $d > a$ Figure 5(b), the receiver lens is entirely away from the center of the cell.

Our goal is to determine the fraction of the transmit power that falls on the receiver lens. To do this, let us consider Figure5(a) first. When $0 \leq r \leq a-d$ the contour with intensity $e_0 e^{-fr^2}$ is contained entirely within the receiver lens. The total signal intensity along such a contour is, $2\pi r e_0 e^{-fr^2}$. If $a - d < r \leq a + d$ then we get the situation illustrated by the contour of radius r_2 in Figure 5(a). In this case, the signal intensity contributed by a contour of radius r is equal to the length of the arc (between points p and q in the figure) multiplied by $e_0 e^{-fr^2}$. Using geometry, we calculate the length of such an arc to be,

$$\gamma(r, a, d) = 2\cos^{-1}\left((r^2 - a^2 + d^2)/(2dr)\right) r$$

Finally, to obtain the signal intensity, we integrate over all values of r,

$$E_{Rx}^{d<a} = \int_0^{a-d} 2\pi r e_0 e^{-fr^2} dr + \int_{a-d}^{a+d} \gamma(r, a, d) e_0 e^{-fr^2} dr \tag{3}$$

By similar reasoning, if the receiver lens is shifted by $d \geq a$ then the expression for signal intensity becomes,

$$E_{Rx}^{d\geq a} = \int_{d-a}^{d+a} \gamma(r, a, d) e_0 e^{-fr^2} dr \tag{4}$$

Finally, we need to determine the value of e_0. Observe from Figure 4 that the beam spreads over a circle of radius A. Using simple geometry, we can write, $A = \frac{ah}{F}$. Since the signal is spread over this area as a Gaussian, we have,

$$P_{Tx} \lambda^2 e^{-sK(f)} = \int_0^A e_0 e^{-fy^2} dy \tag{5}$$

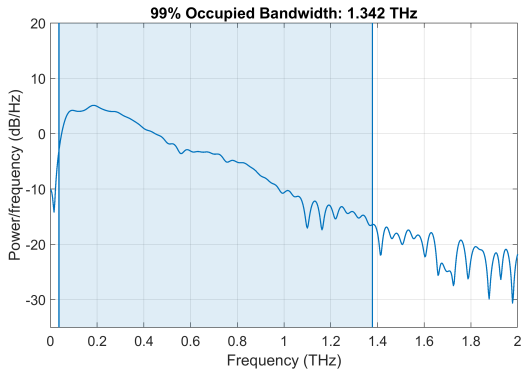

Fig. 6. Received spectrum.

From this expression we immediately obtain e_0 and by combining this value with equations 3 and 4 we obtain the final propagation model as,

$$P_{Rx} = \begin{cases} E_{Rx}^{d<a} P_{Tx} \lambda^2 e^{-sK(f)}, & d < a \\ E_{Rx}^{d \geq a} P_{Tx} \lambda^2 e^{-sK(f)}, & d \geq a \end{cases} \quad (6)$$

III. Measurement and Evaluation of Model

In order to evaluate our coverage model, we utilize extensive measurements conducted in our lab. The equipment we use is a Picometrix T-Ray 4000 Time Domain system, Figure 3. The system produces wideband terahertz pulses by illuminating a silicon crystal with high frequency laser. The resultant signal is then focussed through a HDPE lens. Different types and focal length of lenses can be utilized. For our measurements we used a convex lens. The receiver is synchronized precisely with the transmitter and reverses the process to obtain the pulse. This system has a drawback that the signal strength produced is very low. Therefore, to combat noise effects, we average 10,000 pulses to get one measurement. The Fourier transform of the received pulse is plotted in Figure 6. As we can see, beyond about 1.342 THz, the signal strength becomes very small. Indeed, 99% of the signal strength lies in the band upto 1.342 THz.

For our measurements, we used lenses with focal lengths 1, 3, and 6 inches. The results plotted here correspond to data collected when using the 3 inch lens. We used a value of $h = 8$ cm primarily because the signal strength is so low. To measure the signal strength across the coverage area, we move the receiver lens in small increments perpendicular to the main axis of the transmitter lens. This is called *offset* in the figures. At the receiver we used a *collimating lens* which focuses all parallel rays to the receiver.

We plot the measured received signal power as a function of offset from the lens axis in Figures 7 and 8. We studied the 300 - 370 GHz band in detail since this band covers one of the spectrum windows that is being considered for future small cell deployment. This band is one of the few that is least affected by water in the atmosphere. Figure 7 shows a very good match of our model to measured data. The model diverges from the measured values at high offset values for

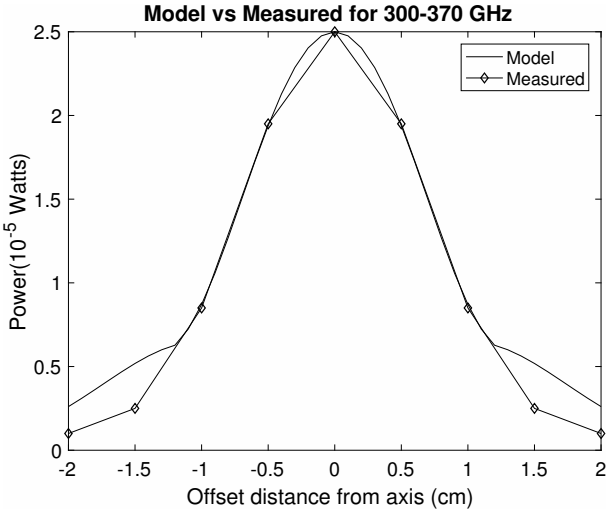

Fig. 7. P_{Rx} for 300-370 GHz channel.

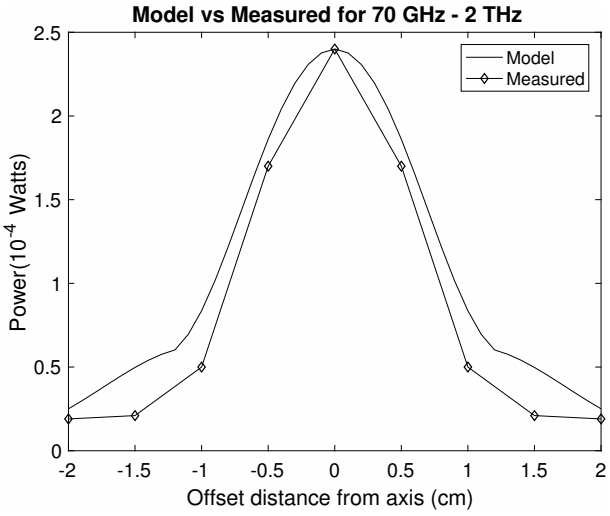

Fig. 8. P_{Rx} for 70 GHz to 2 THz channel.

two reasons. First, signal power is 5x lower at these high offsets as compared with no offset. Furthermore, given that the transmitter has a low power, data at these offsets has a lot of noise and hence variability. The second reason for the mis-match is that the model assumes a perfect Gaussian signal distribution. In reality, this distribution is somewhat different at the edges of coverage. Hence, we see that the model diverges somewhat from measured. Figure 8 shows similar behavior. In this instance, since we are summing over a wide bandwidth, there is more error since the Gaussian distribution as well as point of focus vary depending on the frequency. However, the model does track the measured values very well.

IV. Related Work

For several years, the primary use of terahertz has been for sensing applications (sensing explosives, drugs, etc.) [10], [11]. However, given the rapidly growing demand for bandwidth, the past five years has seen an exponential growth in

research which has led to many companies begin developing hardware to operate at these frequencies. Over the past few years there have been various demonstrations of terahertz communications using *fixed* highly directional antennas with narrow bandwidths and simple modulation schemes such as OOK, ASK, 8PSK etc. For example, Song et al. [12] used 0.25 THz carrier frequency and transmitted 8 Gbit/s error free data over 50cm distance with ASK modulation. Hirata et al. used 0.12 THz carrier frequency and achieved 10 Gbit/s data transmission rate with ASK modulation and forward error correction technique over a distance of 5.8 km [13]. Kallfass et al. [14] chose 0.22 THz carrier frequency with OOK modulation. The authors used electronic techniques with microwave frequency multipliers and achieved data rates up to 40 Gbit/s over a 50 cm distance. In addition to several other demonstrations [15]–[20], most notably Koenig et al. [21] for the first time achieved a data rate as high as 100 Gbit/s over a 20 meter distance between transmitter and receiver. The carrier frequency was 0.237 THz with a bandwidth of 0.035 THz.

In our own previous work [7], [22]–[25], we did detailed measurements of terahertz propagation using the T-Ray system and published the data online at http://terahertz.cs.pdx.edu/. In our papers, we presented a channel model for line-of-sight propagation using collimating lenses. In a more recent paper [26] we presented an initial model for lens-based propagation. however that model was very crude and showed high error. The current model is far more accurate, as is evident from our results in the previous section.

V. Conclusions

This paper presents a detailed channel model for terahertz when using HDPE lenses at the transmitter. We show that the model agrees very well with measured data. This frequency band is virtually unused and therefore can be used to provide very high data rates at short ranges. However, as we show, channel impairments will require careful communication system design. Our future work is looking at more complex signal propagation trajectories (such as reflections) in indoor environments. In addition, we are studying the challenges of resource allocation for terahertz based cells.

References

[1] "Itu-r: Future technology trends of terrestial imt systems," Report ITU-R M.2320-0, November 2014.

[2] I. F. Akyildiz, J. M. Jornet, and C. Han, "Teranets: Ultra-broadband communication networks in the terahertz band," *IEEE Wireless Communications Magazine*, pp. 130 – 135, August 2014.

[3] C. Lin and G. Y. Li, "Indoor terahertz communications: how many antenna arrays are needed?" *IEEE Transactions on Wireless Communications*, vol. 14, no. 6, June 2015.

[4] "Final report from the nsf workshop on future directions in wireless networking," Arlington, VA, Nove,ber 4 – 5 2013.

[5] "Ieee 802.15 wpan terahertz interest group (igthz)," www.ieee802.org/15/pub/IGthzOLD.html, November 12 2015.

[6] H. T. Friis, "A note on a simple transmission formula," *Proceedings of the IRE*, vol. 34, no. 5, pp. 254–256, 1946.

[7] F. Moshir and S. Singh, "Rate adaptation for terahertz communications," in *Proceedings 13th Annual IEEE Consumer Communications & Networking Conference*, Las Vegas, NV, January 9 – 12 2016.

[8] ——, "Modulation and rate adaptation algorithms for terahertz channels," *Nano Communication Networks*, vol. 10, pp. 38–50, 2016.

[9] A. Ghaffar, "Field intensity distribution by a cylindrical plano convex lens placed in a homogenous un-magnetized plasma media," *Journal of Optoelectronics and Advanced Materials*, vol. 17, no. 3-4, pp. 285–289, April 2015.

[10] J. F. Federici, D. Gary, R. Barat, and D. Zimdars, "THz standoff detection and imaging of explosives and weapons," in *Defense and Security*. International Society for Optics and Photonics, 2005, pp. 75–84.

[11] D. Woolard, P. Zhao, C. Rutherglen, Z. Yu, P. Burke, S. Brueck, and A. Stintz, "Nanoscale imaging technology for THz-frequency transmission microscopy," *International Journal of High Speed Electronics and Systems*, vol. 18, no. 01, pp. 205–222, 2008.

[12] H. Song, K. Ajito, A. Hirata, A. Wakatsuki, T. Furuta, N. Kukutsu, and T. Nagatsuma, "Multi-gigabit wireless data transmission at over 200-GHz," in *34th International Conference on Infrared, Millimeter, and Terahertz Waves, 2009. IRMMW-THz 2009*, 2009, pp. 1–2.

[13] A. Hirata, T. Kosugi, H. Takahashi, J. Takeuchi, K. Murata, N. Kukutsu, Y. Kado, S. Okabe, T. Ikeda, F. Suginosita *et al.*, "5.8-km 10-Gbps data transmission over a 120-GHz-band wireless link," in *2010 IEEE International Conference on Wireless Information Technology and Systems (ICWITS),*. IEEE, 2010, pp. 1–4.

[14] I. Kallfass, J. Antes, T. Schneider, F. Kurz, D. Lopez-Diaz, S. Diebold, H. Massler, A. Leuther, and A. Tessmann, "All active MMIC-based wireless communication at 220 GHz," *IEEE Transactions on Terahertz Science and Technology*, vol. 1, no. 2, pp. 477–487, November 2011.

[15] J. Antes, J. Reichart, D. Lopez-Diaz, A. Tessmann, F. Poprawa, F. Kurz, T. Schneider, H. Massler, and I. Kallfass, "System concept and implementation of a mmW wireless link providing data rates up to 25 Gbit/s," in *2011 IEEE International Conference on Microwaves, Communications, Antennas and Electronics Systems (COMCAS)*, Nov 2011, pp. 1–4.

[16] B. Zhang, Y.-Z. Xiong, L. Wang, and S. Hu, "A switch-based ASK modulator for 10 Gbps 135 GHz communication by 0.13 MOSFET," *IEEE Microwave and Wireless Components Letters*, vol. 22, no. 8, pp. 415–417, 2012.

[17] H. Song, K. Ajito, Y. Muramoto, and A. Wakatasuki, "24 Gbit/s data transmission in 300 GHz band for future terahertz communications," *Electronics Letters*, vol. 48, no. 15, pp. 953–954, July 2012.

[18] G. Ducournau, P. Szriftgiser, A. Beck, D. Bacquet, F. Pavanello, E. Peytavit, M. Zaknoune, T. Akalin, and J.-F. Lampin, "Ultrawide-bandwidth single-channel 0.4-THz wireless link combining broadband quasi-optic photomixer and coherent detection," 2014.

[19] C. Wang, C. Lin, Q. Chen, B. Lu, X. Deng, and J. Zhang, "A 10-Gbit/s wireless communication link using 16-QAM modulation in 140-GHz band," *IEEE Transactions on Microwave Theory and Techniques*, vol. 61, no. 7, pp. 2737–2746, July 2013.

[20] B. Lu, W. Huang, C. Lin, and C. Wang, "A 16QAM modulation based 3Gbps wireless communication demonstration system at 0.34 THz band," in *Infrared, Millimeter, and Terahertz Waves (IRMMW-THz), 2013 38th International Conference on*. IEEE, 2013, pp. 1–2.

[21] S. Koenig, D. Lopez-Diaz, J. Antes, F. Boes, R. Henneberger, A. Leuther, A. Tessmann, R. Schmogrow, D. Hillerkuss, R. Palmer, T. Zwick, C. Koos, W. Freude, O. Ambacher, J. Leuthold, and I. Kallfass, "Wireless sub-THz communication system with high data rate," *Nature Photonics*, vol. 7, pp. 977–981, October 2013.

[22] F. Moshir and S. Singh, "Modulation for indoor terahertz communication networks," in *Journal of Nano Communication Networks*, Elsevier (Special Issue on Terahertz Communications), 2015.

[23] ——, "Ultrafast pulsed thz communication," in *Proceedings IEEE PIMRC*, Washington, DC, September 2 – 5 2014.

[24] ——, "Wireless barcodes for tagging infrastructure," in *Proceedings ACM MOBICOM*, Maui, HI, September 7 – 10 2014.

[25] ——, "Pulsed terahertz time-domain communication," in *Proceedings IEEE GLOBECOM*, Austin, TX, December 8 – 12 2014.

[26] A. Mirhosseini and S. Singh, "Modeling line-of-sight terahertz channels using convex lenses," in *IEEE ICC*, Shanghai, China, May 20-25 2019.